Models of interface separation accompanied by plastic dissipation at multiple scales

YUEGUANG WEI and JOHN W. HUTCHINSON

Division of Engineering and Applied Sciences, Harvard University, Cambridge, MA 02138 e-mail: hutchinson@husm.harvard.edu

Received 19 November 1998; accepted in revised form 2 December 1998

Abstract. Two continuum mechanical models of interface fracture for interfaces joining materials where at least one undergoes plastic deformation are reviewed and examined critically. The embedded process zone model (EPZ model) has an adhesive zone, characterized by a work of separation and an interface strength, embedded within a continuum model of the adjoining materials. The SSV model imposes an elastic, plasticity-free layer of prescribed thickness between the interface and the surrounding elastic-plastic continuum. Crack advance requires the work of separation to be supplied by the local elastic crack tip field. The objective of each model is to provide the relation between the macroscopic interface toughness (the total work of fracture) and the work of separation. Under steady-state crack growth, the total work of fracture is the work of separation plus the work of plastic dissipation, the latter often far exceeding the former. It will be argued that each model has its own domain of validity, subject to the accuracy of conventional continuum plasticity at small scales, but neither is able to capture the dramatic trends which have been observed in macroscopic toughness measurements stemming from alterations in interface bonding conditions. A unified model is proposed which coincides with the two models in their respective domains of validity and provides a transition between them. Interface separation energy and interface strength (the peak separation stress) each play a central role in the unified model. Strain gradient plasticity is used to illustrate the effect of plastic deformation at the micron scale on the link between interface and macroscopic properties.

Key words: Adhesion, fracture, interface strength, interface toughness, plasticity.

1. Introduction

Linking the fracture process to macroscopic fracture behavior

A zone of plasticity will generally surround the fracture process governing separation at a bi-material interface if at least one of the materials is a metal or polymer. Under quasi-static, steady-state propagation, the macroscopic toughness of the interface (the total work of fracture) is the sum of the work of separation and the plastic dissipation. Plastic dissipation contributes a large fraction of the macroscopic toughness for many interfaces. This paper examines mechanics models which relate the macroscopic work of fracture to the work of separation. Specifically, the embedded fracture process zone model (EPZ model) of Needleman (1984) and Tvergaard and Hutchinson (1992, 1993) and the plasticity-free strip model (SSV model) of Suo, Shih and Varias (1993) and Beltz et al. (1996) will be discussed with emphasis on delineating their domains of validity. A unified model will be proposed which coincides with the two models in their respective domains of validity and provides a transition between them.

In attempts to bridge from the microscopic to macroscopic scales in interface fracture, there is an important distinction that must be drawn between different classes of fracture processes (Evans et al., 1998). Where interface adhesion is controlled by atomic or molecular

separation, the continuum plasticity description must give adequate estimates of stresses and plastic dissipation over the full range of scales for which it is used in the model. In particular, it must be capable of providing stresses at the micron to sub-micron scale, where conventional plasticity theory becomes suspect. There are important fracture processes (void nucleation, growth and coalescence in metals and crazing in polymers) which control separation on a scale measured in tens of microns or more. In these cases, conventional macroscopic plasticity theory is adequate to link all the way to the fracture process. The scale of the fracture process is consequently of essential importance in setting the requirements on the plasticity description used in fracture models.

Prior to detailing the three models, we begin by listing the parameters which appear in the models, indicating typical values for separation processes occurring at the at atomic or molecular scale and for those such as void growth which occur at larger scales. The thrust of the paper will be on adhesion models for separation processes occurring on the atomic or molecular scale.

Interface parameters

The primary parameters used to characterize separation of interfaces are the work of separation, Γ_0 , and the peak separation stress $\hat{\sigma}$, which will also be referred to as the interface strength. The critical separation of the two materials on either side of the interface when the traction stress has dropped to zero δ_c , is not an independent parameter because $\Gamma_0 \propto \hat{\sigma} \delta_c$, where the constant of proportionality depends of the shape of the traction-separation law. For atomic separation of a moderately strong metal/ceramic interface (Raynolds et al., 1996)

$$\Gamma_0 \approx 1 \, \mathrm{Jm}^{-2}, \qquad \hat{\sigma} \approx 10 \, \mathrm{GPa}, \qquad \delta_c \approx 10^{-10} \, \mathrm{m}.$$
 (1.1)

The range of the separation parameters can be very large when the fracture process at a metal/ceramic interface is void nucleation, growth and coalescence within the metal. A representative set of values is

$$\Gamma_0 \approx 1 \, \mathrm{kJm}^{-2}, \qquad \hat{\sigma} \approx 1 \, \mathrm{GPa}, \qquad \delta_c \approx 1 \, \mu \mathrm{m}.$$
 (1.2)

The scale of the process is set by the spacing between voids or void-nucleating particles in the metal at the interface. Most of work of the separation is plastic deformation consumed in the growth and coalescence of the voids on the fracture plane. Separation involving crazing at a strong interface between a polymer and a metal or ceramic can also lead to values such as (1.2), usually with somewhat smaller interface strengths and critical separations correspondingly larger.

The SSV model for atomic or molecular adhesive separation invokes an elastic layer of thickness D from which plastic deformation is excluded lying between the plastic zone and the interface. This length quantity can be regarded as a material fitting parameter (Suo et al., 1993), or it can be estimated using dislocation concepts (Beltz et al., 1996; Lipkin et al., 1996). Typically, values are found to fall in the range

$$D \approx 10$$
 to $100 \,\mathrm{nm}$. (1.3)

Continuum parameters

The parameters employed in the most widely used continuum theories for elastic-plastic solids are Young's modulus E, Poisson's ratio ν , yield stress in uniaxial tension σ_Y , and strain hardening exponent N. The J_2 flow theory of plasticity characterizing initially isotropic solids undergoing isotropic strain hardening has been used in nearly all the modeling thus far, and it will be used here as well for the studies based on 'conventional' theory. Conventional theories give an adequate description of plastic deformation as long as the scale of deformation field is somewhat above a micron. Experiments (hardness tests, wire torsion, film bending) conducted at the micron to sub-micron scale reveal much higher stresses at a given level of deformation than conventional plasticity would suggest. The conventional theories fail to account for significant elevations in strain hardening when small scale plastic deformation occurs in the presence of strain gradients. Deformations at the micron to sub-micron scale typically involve large numbers of dislocations such that a continuum approach retains its advantages over dislocation mechanics. The strong size effect requires the introduction of a material length scale ℓ into the constitutive law. In this paper, the strain gradient plasticity generalization of J_2 flow theory of Fleck and Hutchinson (1997) will be employed to illustrate the influence of the plasticity length parameter ℓ in fracture modeling.

Plastic zone sizes

There are two length quantities related to the size of the plastic zone for a bi-material interface crack (Tvergaard and Hutchinson, 1993)

$$R_0 = \frac{2}{3\pi (1 - \nu^2)(1 - \beta_D^2)} \left[1 + \frac{(1 - \nu_s^2)E}{(1 - \nu^2)E_s} \right]^{-1} \frac{E\Gamma_0}{\sigma_Y^2},$$
 (1.4a)

$$R_{ss} = \frac{2}{3\pi (1 - \nu^2)(1 - \beta_D^2)} \left[1 + \frac{(1 - \nu_s^2)E}{(1 - \nu^2)E_s} \right]^{-1} \frac{E\Gamma_{ss}}{\sigma_Y^2},$$
 (1.4b)

where E, ν and σ_Y pertain to the plastically deforming material, E_s and ν_s pertain to the elastic material, and β_D is the second Dundurs elastic mismatch parameter which will be given later. Here, Γ_{ss} denotes the total steady-state work of fracture (i.e. the remote energy release rate under small scale yielding conditions), and R_{ss} is a rough estimate (to within a factor of about 2) of the size of the active plastic zone at the crack tip. Both Γ_{ss} and R_{ss} are computed quantities, unknown in advance. The length quantity R_0 is fundamental and appears prominently in all the models: it is specified in terms of the model parameters. By (1.4), R_0 can be thought of as the size of the plastic zone if the remote energy release rate were Γ_0 . In other words, R_0 would be the size of the active plastic zone if the total work of fracture were not much larger than Γ_0 . By (1.4), the two length quantities are related by $R_{ss}/R_0 = \Gamma_{ss}/\Gamma_0$. In the absence of elastic mismatch between the two materials, $R_0 = [3\pi(1-\nu^2)]^{-1}(E\Gamma_0/\sigma_Y^2)$.

For metal-ceramic interfaces undergoing atomic separation $\Gamma_0 \approx 1 \, \mathrm{Jm}^{-2}$, and, typically

$$R_0 = 0.1$$
 to $1 \,\mu\text{m}$. (1.5)

If separation occurs by the ductile void growth mechanism $\Gamma_0 \approx 1 \, \text{kJm}^{-2}$, and

$$R_0 = 0.1$$
 to 1 mm. (1.6)

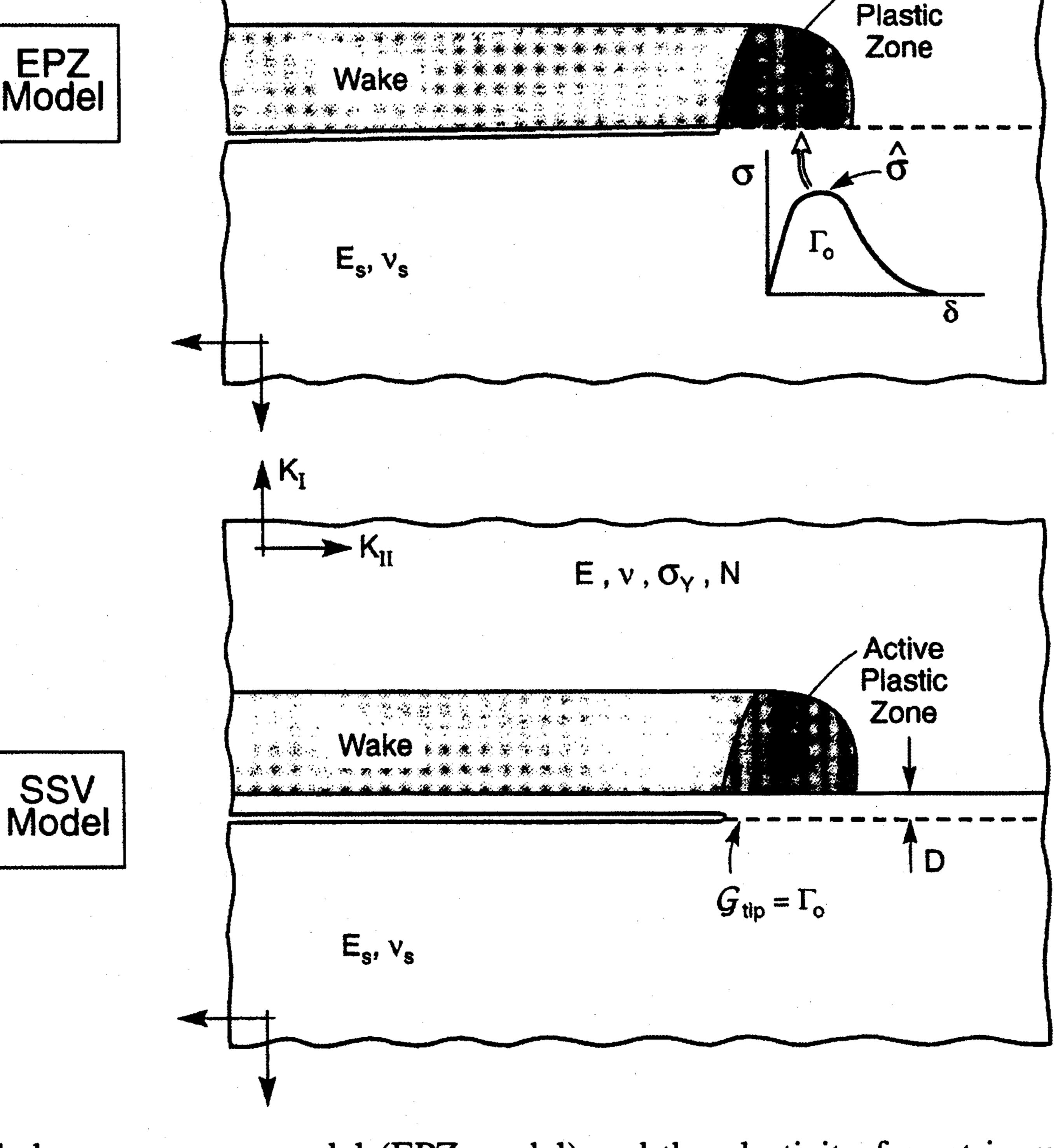


Figure 1. The embedded process zone model (EPZ model) and the plasticity-free strip model (SSV model) for a bi-material interface where the upper material is elastic-plastic and the lower material is elastic. The study is limited to steady-state crack growth in small scale yielding wherein the active plastic zone is small compared to the crack length. The finite length crack is replaced by a semi-infinite crack loaded remotely by the elastic K-field.

The plastic zone size R_{ss} can be as small as R_0 if plastic dissipation is negligible, or it can be as much as 100 or more times R_0 when plastic dissipation is pronounced.

2. EPZ and SSV models

The embedded fracture process zone model (EPZ model) and the plasticity-free strip model (SSV model) share a number of common features. Both provide a link from interface separation to be the macroscopic scale using continuum descriptions of the elastic-plastic solids joined at the interface. Both aim to elucidate the role of plastic dissipation in amplifying the macroscopic toughness above the work of interface separation. The difference between the two models lies in the local separation criterion proposed for the interface.

The two models are shown in Figure 1 for the case where the material above the interface is elastic-plastic and that below is elastic. Plane strain conditions are assumed for both models. Moreover, in this paper, attention is restricted to small scale yielding wherein the plastic zone at the crack tip is sufficiently small compared to the crack length itself such that the asymptotic problem can be considered for two half spaces with a semi-infinite crack along the interface. The remote loading is prescribed using the stress intensity factors, K_1 and K_2 , for the crack tip field of the elastic bi-material problem (Rice, 1988). That field has tractions on the interface specified by

$$\sigma_{22} + i\sigma_{12} = (K_1 + iK_2)(2\pi r)^{-1/2}r^{-i\varepsilon}, \qquad (2.1)$$

where r is the distance from the tip and $i = \sqrt{-1}$. The so-called oscillation index is given by

$$\varepsilon = \frac{1}{2} \ln \left(\frac{1 - \beta_D}{1 + \beta_D} \right), \tag{2.2}$$

where β_D is the second Dundurs' mismatch parameter

$$\beta_D = \frac{1}{2} \frac{\mu(1 - 2\nu_s) - \mu_s(1 - 2\nu)}{\mu(1 - \nu_s) + \mu_s(1 - \nu)}$$
(2.3)

and μ and μ_s are the shear moduli of the upper and lower materials. The remote, or macroscopic, energy release is

$$G = \frac{1}{2}(1 - \beta_D^2) \left(\frac{1 - \nu^2}{E} + \frac{1 - \nu_s^2}{E_s}\right) (K_1^2 + K_2^2). \tag{2.4}$$

When $\varepsilon \neq 0$, the definition of mode mixity requires that a choice of distance L ahead of the tip be made at which the relative amount of shear stress to normal stress acting on the interface is determined

$$\tan \psi = \frac{\sigma_{12}}{\sigma_{22}} = \frac{\text{Im}[(K_1 + i K_2) L^{i\varepsilon}]}{\text{Re}[(K_1 + i K_2) L^{i\varepsilon}]}.$$
(2.5)

This reduces to $\tan \psi = K_2/K_1$ if $\beta_D = 0$. The choice $L = R_{ss}$ is used the present study. The displacement components associated with the elastic bi-material singularity field are given by Rice et al. (1990) (see also, Tvergaard and Hutchinson, 1993).

In studies conducted until now, the conventional J_2 flow theory of plasticity has been used to characterize deformation in the upper half space. This isotropic hardening theory is based on the von Mises, or J_2 , yield surface. The small strain version of the theory is employed, consistent with the fact that the strains at the tip of the steadily growing crack are indeed relatively small under conditions in which interface separation occurs. The tensile stress-strain relation used in the present study to represent the upper half space is

$$\varepsilon = \sigma/E$$
 for $\sigma \leqslant \sigma_Y$,
 $= (\sigma_Y/E)(\sigma/\sigma_Y)^{1/N}$ for $\sigma > \sigma_Y$, (2.6)

where E is its Young's modulus and ν its Poisson's ratio. This information fully specifies J_2 flow theory. The lower half space is elastic with isotropic properties characterized by E_s and ν_s .

Conventional plasticity theories fail to account for important size-dependencies at small length scales (Fleck et al., 1994; Fleck and Hutchinson, 1997; Nix and Gao, 1998). Specifically, strain hardening is significantly elevated above the predictions of conventional plasticity when plastic deformation occurs at the micron to sub-micron scale in the presence of strain gradients. A crack tip induces strong strain gradients, and it is reasonable to expect that a zone

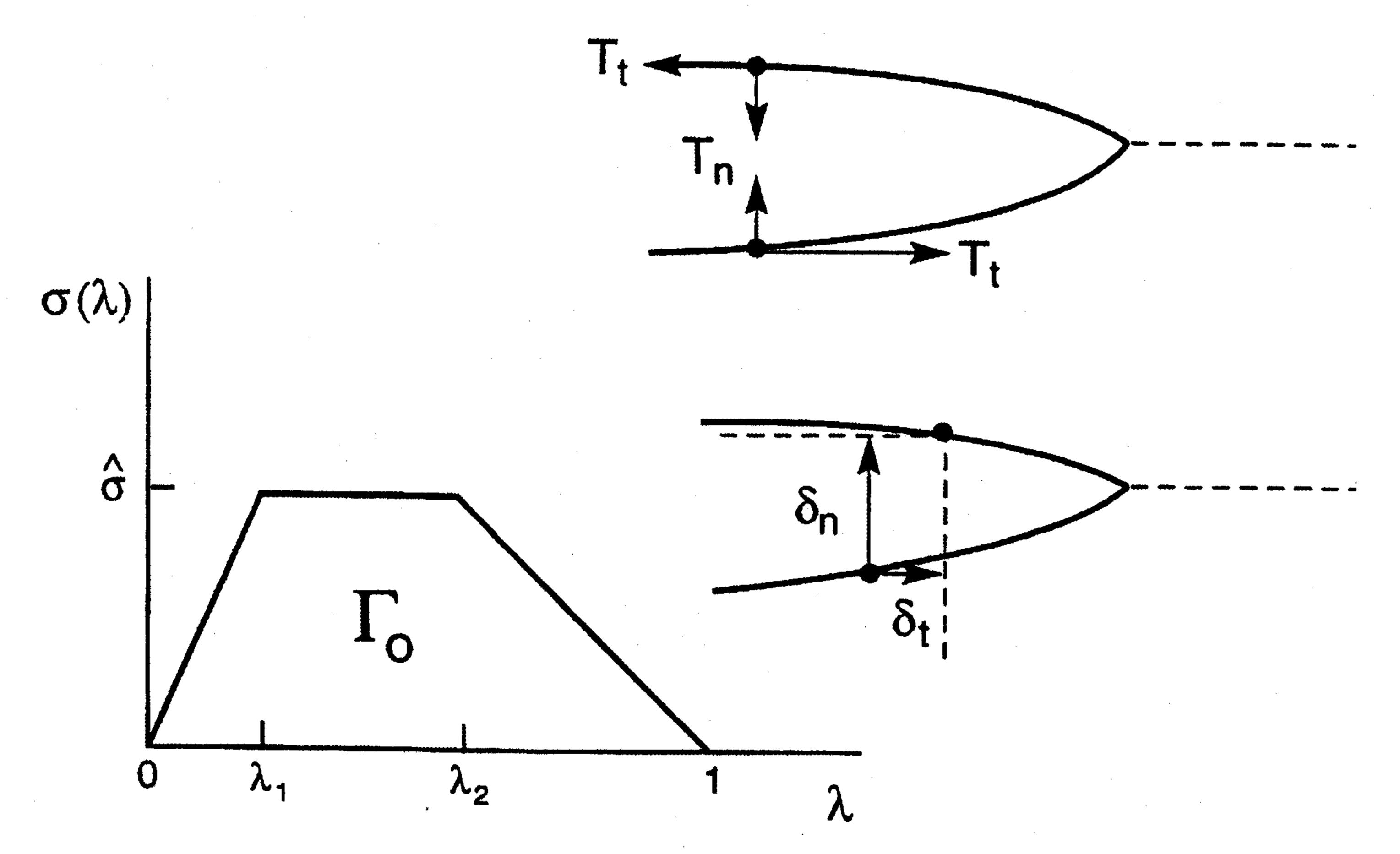


Figure 2. The traction-separation behavior characterizing the interface in the EPZ model and the unified model.

of gradient hardened material surrounds the crack tip. The associated traction elevation on the interface may significantly affect the link between macroscopic toughness and microscopic interface separation, particularly when the interface is strong. This connection will be explored in Section 4 where a strain gradient theory of plasticity will be substituted for J_2 flow theory to describe the upper half space.

The above specifications are common to all of models considered in this paper, including the unified model. Details specific to the individual models are now addressed.

2.1. THE EPZ MODEL

In the EPZ model a traction-separation law characterizing the interface fracture process is embedded as an internal boundary condition along the interface. In the present applications of the model, the fracture process zone along the interface lies between the plastic zone on one side of the interface and elastic material on the other. Once the parameters of the separation law are specified, the model can be used to compute the relation between crack advance and G. The primary quantity of interest here is the steady-state interface toughness Γ_{ss} , which is identified with the computed value of remote energy release rate G in (2.4) needed to advance the crack in small scale yielding under steady-state conditions.

Following the notation for the law introduced in Tvergaard and Hutchinson (1993), let δ_n and δ_t be the normal and tangential components of the relative displacement of the crack faces across the interface, as indicated in Figure 2. Let δ_n^c and δ_t^c be critical values of these displacement components, and define a single dimensionless separation measure as

$$\lambda = \sqrt{(\delta_n/\delta_n^c)^2 + (\delta_t/\delta_t^c)^2},\tag{2.7}$$

such that the tractions drop to zero when $\lambda = 1$. With $\sigma(\lambda)$ displayed in Figure 2, a potential from which the tractions are derived is defined as

$$\Phi(\delta_n, \delta_t) = \delta_n^c \int_0^{\lambda} \sigma(\lambda') \, d\lambda'. \tag{2.8}$$

The normal and tangential components of the traction acting on the interface in the fracture process zone are given by

$$T_n = \frac{\partial \Phi}{\partial \delta_n} = \frac{\sigma(\lambda)}{\lambda} \frac{\delta_n}{\delta_n^c}, \qquad T_t = \frac{\partial \Phi}{\partial \delta_t} = \frac{\sigma(\lambda)}{\lambda} \frac{\delta_t}{\delta_t^c} \frac{\delta_n^c}{\delta_t^c}. \tag{2.9}$$

The traction law under a purely normal separation $(\delta_t = 0)$ is $T_n = \sigma(\lambda)$ where $\lambda = \delta_n/\delta_n^c$. Under a purely tangential displacement $(\delta = 0)$, $T_t = (\delta_n^c/\delta_t^c)\sigma(\lambda)$ where $\lambda = \delta_t/\delta_t^c$. The peak normal traction under purely normal separation is $\hat{\sigma}$, and the peak shear traction is $(\delta_n^c/\delta_t^c)\hat{\sigma}$ in a purely tangential 'separation'. The work of separation per unit area of interface Γ_0 is given by (2.8) with $\lambda = 1$. For the separation function $\sigma(\lambda)$ specified in Figure 2,

$$\Gamma_0 = \frac{1}{2}\hat{\sigma}\delta_n^c [1 - \lambda_1 + \lambda_2]. \tag{2.10}$$

The parameters governing the separation law of the interface are the work of the fracture process Γ_0 , the peak stress $\hat{\sigma}$, and the critical displacement ratio δ_n^c/δ_t^c , together with the factors λ_1 and λ_2 governing the shape of the separation function. Note that use of the potential ensures that the work of separation is Γ_0 regardless of the combination of normal and tangential displacements taking place in the process zone. Experience gained in the earlier studies suggests that the details of the shape of the separation law are relatively unimportant. The two most important parameters characterizing the fracture process in this model are Γ_0 and $\hat{\sigma}$. The parameter δ_n^c/δ_t^c is the next most important, but the study of mixed mode interface toughness using this model (Tvergaard and Hutchinson, 1993) indicates that predictions are relatively insensitive to this parameter except when the loading is dominantly mode II. Then the peak in the shearing stress controls separation, and δ_n^c/δ_t^c becomes important.

The condition for crack advance is attainment of $\lambda = 1$ at the current end of the traction-separation zone. In steady-state propagation, this condition must be imposed on the solution.

2.2. THE SSV MODEL

One limitation of the EPZ model as specified above is its failure to provide realistic predictions when the peak interface separation stress $\hat{\sigma}$ is prescribed to be at levels required for separation of strong interfaces, as will be evident from the numerical results described subsequently. In part, this limitation appears to be a consequence of the inadequacy of conventional plasticity to account for stress elevation in the region of high strain gradients at the tip of the crack (Wei and Hutchinson, 1997). Limitations of the EPZ model will be further discussed in Section 3 and 4. At this point, however, they serve to motivate the rationale for the SSV model. Under the assumption that dislocations emitted at the crack tip play a minimal role in crack propagation for the class of interfaces under study, Suo, Shih and Varias (1993) proposed a model capable of producing the high stresses at the crack tip necessary for atomic separation. They imposed an elastic, plasticity-free layer between the interface and the plastic zone. For the case in which the upper half space is elastic-plastic, a layer of thickness D with the same elastic properties as the upper material is inserted above the interface, as shown in Figure 1. Thus, the interface crack tip lies fully within an elastic bi-material region and experiences stress intensity factors $K_{\rm I}^{\rm tip}$ and energy release rate

$$G_{\text{tip}} = \frac{1}{2}(1 - \beta_D^2) \left(\frac{1 - \nu^2}{E} + \frac{1 - \nu_s^2}{E_s}\right) (K_{\text{I}}^{\text{tip}^2} + K_{\text{II}}^{\text{tip}^2}). \tag{2.11}$$

In this model, there is no explicit recognition of an interface separation law. Because the tractions on the interface are unbounded as the tip is approached, it is tacitly assumed that the length of any separation zone would be sufficiently small compared to D such that the peak interface separation stress $\hat{\sigma}$ will always be attained. Thus, $\hat{\sigma}$ is not a parameter in this model. The criterion for crack propagation is simply $G_{\text{tip}} = \Gamma_0$, where Γ_0 is the local work of interface separation. Mode mixity effects could be introduced at this local level, but in this study Γ_0 will be taken to be mode-independent, as has been done in the case of the EPZ model.

The problem for the steady-state SSV model involves the computation of G_{tip} as a function of the continuum properties of the two materials D, the remote energy release rate $G \equiv \Gamma_{ss}$, and ψ . The condition $G_{\text{tip}} = \Gamma_0$ is imposed to obtain Γ_{ss}/Γ_0 . In passing, it can be mentioned that Tvergaard (1997) has shown for the mode I problem that replacing the strip by a circular elastic region with radius D centered at the tip, results in little change in the predictions of the SSV model.

2.3. Γ_{ss}/Γ_0 FROM THE EPZ AND SSV MODELS

For the EPZ model, dimensional considerations dictate that Γ_{ss}/Γ_0 must have a functional dependence of the form

$$\frac{\Gamma_{ss}}{\Gamma_0} = F_{\text{EPZ}} \left\{ \frac{\hat{\sigma}}{\sigma_Y}, N, \psi \right\}. \tag{2.12}$$

There is also some dependence on the moduli ratio E/E_s , the Poison ratios, and the dimensionless parameters λ_1 , λ_2 and δ_n^c/δ_t^c , characterizing the details of the traction-separation law for the interface. However, the most important variables influencing Γ_{ss}/Γ_0 are those displayed explicitly in (2.12). It can be shown that (2.12) is otherwise independent of σ_Y/E . The dependence on the critical separation displacement δ_n^c , is fully accounted for by the choice of dimensionless variables listed.

Apart from the elastic layer thickness D in the SSV model, the fundamental length parameter in both models is R_0 defined in (1.4a). For the SSV model, the most important variables determining Γ_{ss}/Γ_0 are

$$\frac{\Gamma_{ss}}{\Gamma_0} = F_{SSV} \left\{ \frac{R_0}{D}, N, \psi \right\}. \tag{2.13}$$

To set the stage for numerical results presented later in the paper, results are first presented for steady-state, mode I ($\psi = 0$) growth in a homogeneous elastic-plastic material (2.6). Curves of Γ_{ss}/Γ_0 as a function of $\hat{\sigma}/\sigma_Y$ for the EPZ model (Tvergaard and Hutchinson, 1992) and as a function of R_0/D for the SSV model (Suo et al., 1993) are plotted in Figure 3 for three values of the strain hardening exponent N. In this case, the SSV model has a plasticity-free layer of total thickness 2D symmetrically located about the extended crack line.

From Figure 3 it can be noted that the ratio R_0/D , specifying the thickness of the plasticity-free layer in the SSV model plays a role similar to the normalized separation strength $\hat{\sigma}/\sigma_Y$, in the EPZ model. When based on conventional plasticity theory, the EPZ model is limited to values of normalized separation strength $\hat{\sigma}/\sigma_Y$ less than 4 or 5, depending on N (c.f. Figure 3). At higher separation strengths, the stress levels achieved on the extended crack plane are not high enough to produce separation, and crack growth will not occur. By contrast, it will be seen that the SSV model becomes invalid at low separation strengths (at a given Γ_0) because

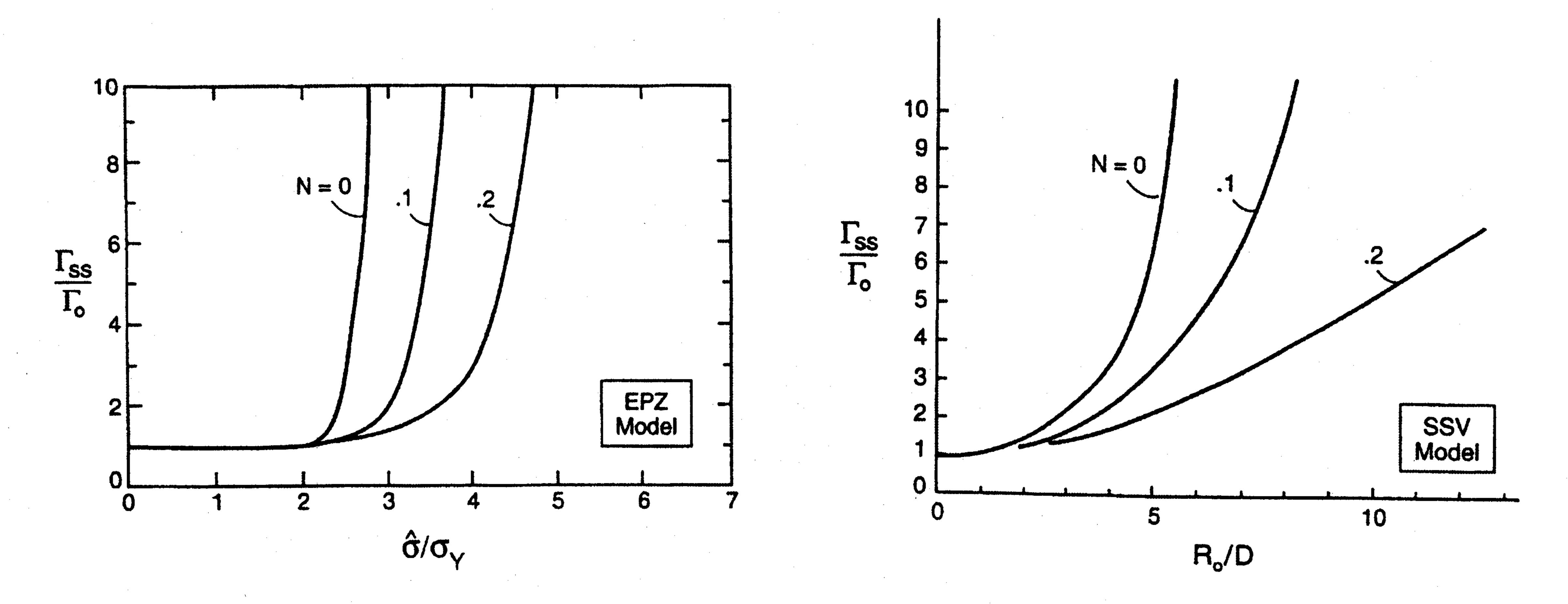


Figure 3. The ratio of steady-state macroscopic work of fracture to work of separation Γ_{ss}/Γ_0 , for the EPZ and SSV models specialized to mode I growth in a homogeneous elastic-plastic solid. The EPZ results are from Tvergaard and Hutchinson (1992) with $\nu = 0.3$, $\lambda_1 = 0.15$ and $\lambda_2 = 0.5$. The SSV results are from Suo et al. (1993) with $\nu = 0.3$.

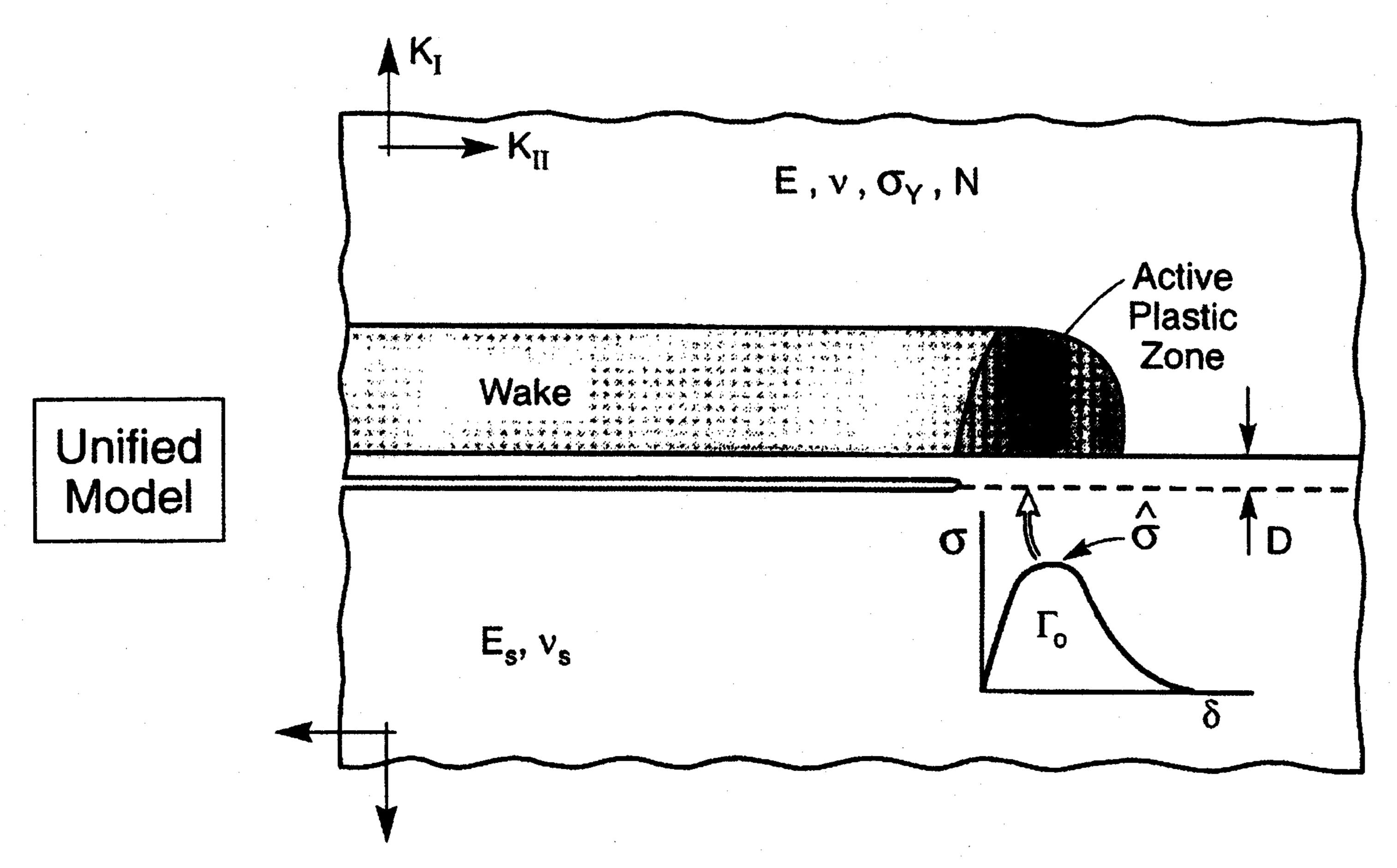


Figure 4. The unified model for crack growth along a bi-material interface under small scale yielding. The model incorporates the plasticity-free strip from the SSV model and the embedded traction-separation characterization of the interface from the EPZ model.

the length of the separation zone at the interface becomes comparable to or even larger than D. Then, the justification for tacitly assuming attainment of the peak separation stress in the SSV model is violated.

3. Unified model

Neither of the two models just discussed is capable of spanning the large observed variations in steady-state macroscopic toughness brought about by the effect of deleterious interface segregants on interface adhesion energy and strength (Evans et al., 1998). A unified model includes the respective limits of the two models and spans a much larger range of possible behaviors. The unified model (Figure 4) incorporates both the traction-separation description (2.9) of the interface used in the EPZ model and the plasticity-free layer of thickness D of

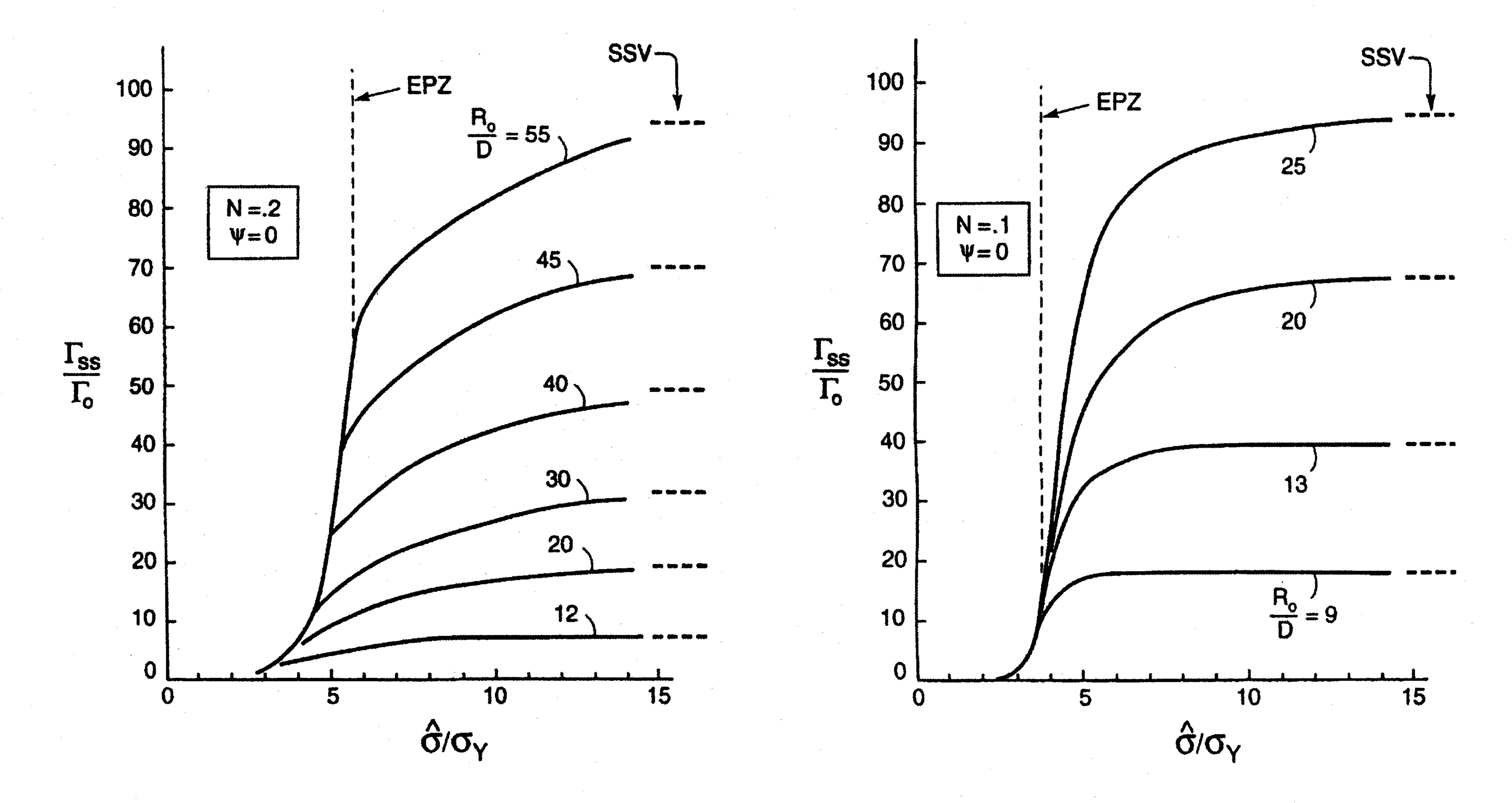


Figure 5. The ratio of the macroscopic work of fracture to work of separation, Γ_{ss}/Γ_0 , for the unified model for mode I ($\psi = 0$) steady-state crack growth along a bi-material interface joining an elastic-plastic solid to a rigid solid. The parameters used in carrying out the calculations are $\nu = 0.3$, $\lambda_1 = 0.15$, $\lambda_2 = 0.5$ and $\delta_n^c/\delta_t^c = 1$.

the SSV model. The interface is characterized by the adhesion energy and strength Γ_0 and $\hat{\sigma}$, and the plasticity-free zone of width D. Consequently, the unified model has one more parameter than either of the other two models. As in the case of the SSV model, D will again be regarded here as a material modeling parameter. For the unified model the set of the most important nondimensional variables on which Γ_{ss}/Γ_0 depends is

$$\frac{\Gamma_{ss}}{\Gamma_0} = F_{\text{UNIFIED}} \left\{ \frac{\hat{\sigma}}{\sigma_Y}, \frac{R_0}{D}, N, \psi \right\}. \tag{3.1}$$

The additional parameters cited just beneath (2.12) are again relevant but continue to be less important than those identified in (3.1).

The numerical method used to generate solutions to the steady-state unified model is the same as that discussed in detail elsewhere for the EPZ model (Wei and Hutchinson, 1997). The same method has been used to solve the SSV model. Plastic deformation in crack growth problems is strongly history dependent. As depicted in Figure 4, an active plastic zone travels with the crack tip leaving behind a wake of residual plastic strains. The field equations are highly nonlinear. A finite element formulation is employed and iteration is used to directly achieve the steady-state solution.

Calculations have been performed to determine the functional dependencies in (3.1) for the case of mode I loading ($\psi = 0$) for a bi-material combination where the lower half-space is rigid ($E_s/E \to \infty$). For this case, the second Dundurs parameter reduces to

$$\beta_D = \frac{-(1-2\nu)}{2(1-\nu)} = -0.286 \text{ (for } \nu = 0.3).$$
 (3.2)

The results are plotted in Figure 5 in the form of Γ_{ss}/Γ_0 as a function of $\hat{\sigma}/\sigma_Y$ at fixed values of R_0/D . Included in each of these figures as a dashed curve is the result for the EPZ

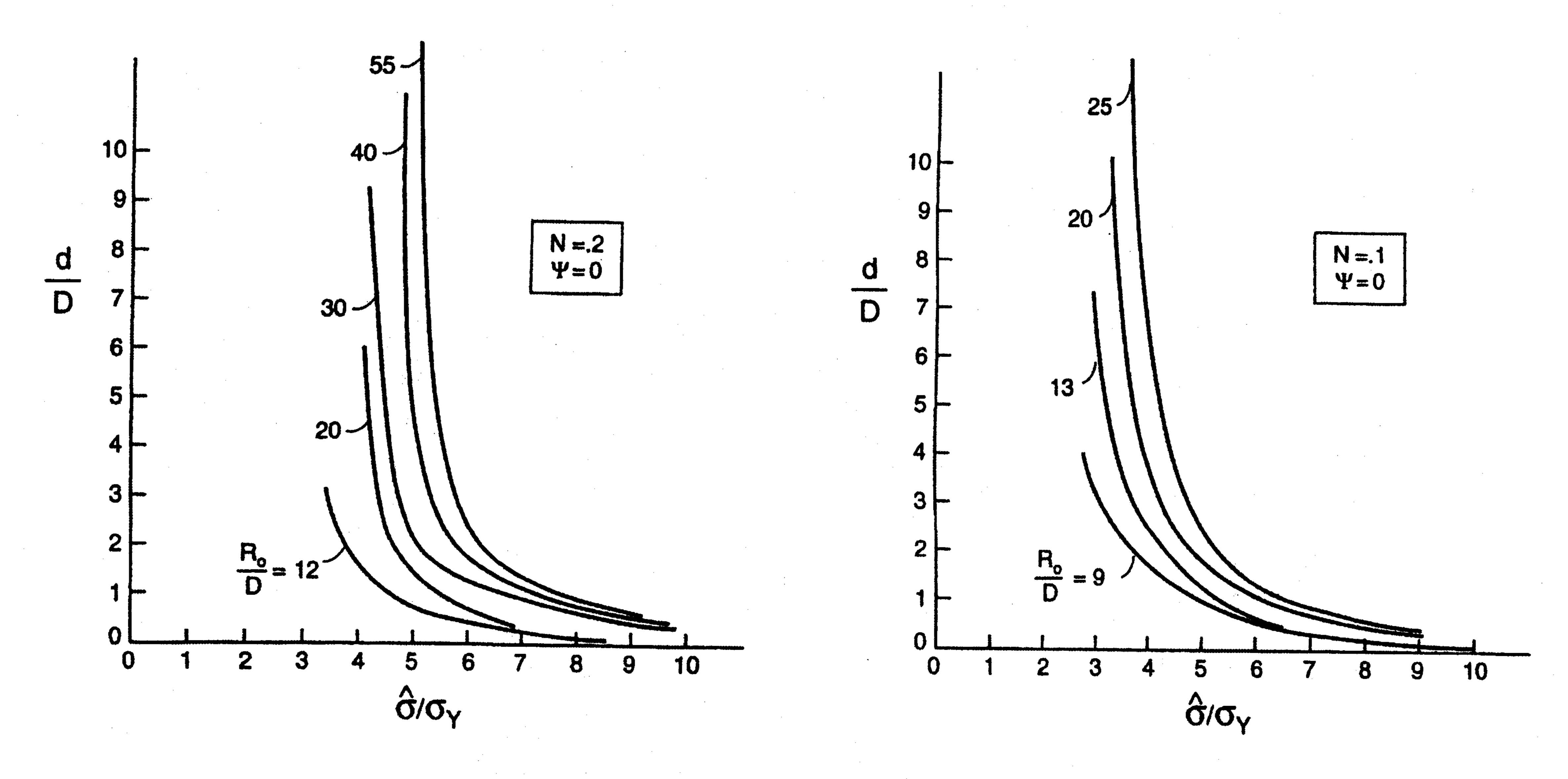


Figure 6. The ratio of the length of the separation zone at the interface to the thickness of the plasticity-free strip d/D, for the examples of Figure 5.

model. The limit corresponding to the SSV model is also indicated for each value of R_0/D . Recall that D is not a parameter in the EPZ model, nor does $\hat{\sigma}$ appear in the SSV model. It is evident from the results in Figure 5 that the unified model reduces to the two earlier models in special limits and provides a transition between the two models in the intermediate range of parameters. Specifically, the unified model approaches the EPZ model in the limit of large R_0/D as long as $\hat{\sigma}/\sigma_Y$ is within the range for which the EPZ model predicts crack advance. If $\hat{\sigma}/\sigma_Y$ lies outside this range, Γ_{ss}/Γ_0 is unbounded as R_0/D becomes large. The unified model approaches the SSV model for large $\hat{\sigma}/\sigma_Y$ at all values of R_0/D .

The two limits to the unified model are readily understood in terms of the following considerations. First consider the approach to the EPZ model as R_0/D becomes large. Suppose all parameters are fixed except D, which becomes small. Then the traction along the interface within the elastic strip will be approach the stresses imposed on it by the surrounding plastic zone. This limiting situation becomes identical to the EPZ model. Next, consider the approach to the SSV model. Now, suppose all parameters are fixed except $\hat{\sigma}$ and that it becomes large. At fixed Γ_0 , the critical separation δ_n^c is inversely proportional to $\hat{\sigma}$. Thus, as $\hat{\sigma}$ becomes large the length of the separation zone decreases and the separation zone lies more deeply within the elastic strip. This is the situation envisioned in the formulation of the SSV model. Interface tractions can become arbitrarily large near the tip, and $\hat{\sigma}$ no longer plays a controlling role.

Further insight can be had by examining the ratio of the length of the separation zone at the interface d, to the thickness of the elastic strip D. The length of the separation zone is not known in advance and must be computed. For present purposes, it is defined as the distance d along the interface from the point where the peak stress is first attained (i.e. where λ in (2.7) attains λ_1) to the point of separation where $\lambda = 1$ (c.f. Figure 2). Figure 6 presents d/D as a function of $\hat{\sigma}/\sigma_Y$ for the unified model for the same values of R_0/D and N taken above. It is evident that the tacit requirement of the SSV model, that d/D be small, is only achieved for relatively large $\hat{\sigma}/\sigma_Y$. Conversely, at lower $\hat{\sigma}/\sigma_Y$, d/D becomes large, and the presence of the elastic strip in the model become irrelevant such that the EPZ limit applies.

4. The influence of strain gradient plasticity on Γ_{ss}/Γ_0

Steep strain gradients in the vicinity of the crack tip produce a high density of geometrically necessary dislocations and anomalously high levels of strain hardening. The effect has been observed to result in stress amplifications at the micron scale in indentation tests, in torsion of wires and in bending of thin films (Fleck and Hutchinson, 1997). Stress levels have been observed to be as much as two to three times stresses at comparable strains in the absence of strain gradients. Stress elevations of this magnitude are expected to have a profound influence on interface separation. Under circumstances where the length of the separation zone is less than a micron, the separation zone will be surrounded by plastically deformed material which has undergone gradient hardening. Remote loading levels, as measured by Γ_{ss}/Γ_0 , needed to attain the peak separation stress on the interface will be correspondingly lower.

The effect of strain gradient plasticity on the predictions of the EPZ model has been explored by Wei and Hutchinson (1997) for mode I crack growth in homogeneous elastic-plastic solids. That study employed the EPZ model as specified in Section 2.1 with identical elastic-plastic material properties prescribed for the upper and lower half-spaces. A strain gradient theory of plasticity was substituted for the conventional J_2 flow theory as the continuum description of the solid. Lipkin, Clarke and Beltz (1996) introduced strain gradient hardening into a version of the SSV model specialized to the onset of crack growth rather than steady-state growth. Their approach leads to the identification of D as the distance from the tip where the stresses arising from strain gradient hardening merge continuously with those in the plasticity-free strip.

The strain gradient theory which will be used here is the same as that employed in the earlier EPZ study. It is a generalization of conventional plasticity theory that reduces to J_2 theory, both when strain gradients vanish or when the scale of the nonuniform deformation is larger than the constitutive length parameter ℓ . In the generalized theory, the constitutive length parameter enters through strain gradient contributions to an effective strain quantity defined as

$$E_e^2 = \varepsilon_e^2 + \ell_{SG}^2 \eta_{ijk}^{(1)} \eta_{ijk}^{(1)} + \frac{2}{3} \ell_{RG}^2 \chi_{ij}' \chi_{ij}', \tag{4.1}$$

where ε_e is the standard Mises effective strain, $\eta_{ijk}^{(1)}$ is a particular combination of the strain gradients which includes both stretch and rotation gradients, and χ_{ij}' is the rotation gradient (Fleck and Hutchinson, 1997). Rotation gradients (ℓ_{RG}) are found to have relatively little influence on the crack tip stresses. The most important strain gradient contribution for the crack growth problem is that involving stretch gradients (ℓ_{SG}). In the present calculations, as well as in those reported by Wei and Hutchinson (1997), the choice $\ell_{SG} = \ell_{RG} \equiv \ell$ has been made, but the value assigned to ℓ_{RG} has relatively little effect on the results. Indentation is ideally suited for the measurement of ℓ_{SG} because it too is relatively insensitive to rotation gradients. Fitting indentation test data for a variety of metals (e.g. Ma and Clarke, 1995; Poole et al., 1996; Stelmashenko et al., 1993) with indentation predictions based on J_2 SGP theory suggests that ℓ_{SG} usually falls within the range from 0.25 to 1 μ m (Begley and Hutchinson, 1998). (Wire torsion and film bending are dominated by rotation gradients and are insensitive to ℓ_{SG} . From such tests, it is inferred that ℓ_{RG} is about 4 or 5 μ m.) Full details of the J_2 SGP theory are given by Fleck and Hutchinson (1997) and by Wei and Hutchinson (1997), who provide formulas for the incremental version of the theory used in the crack growth models.

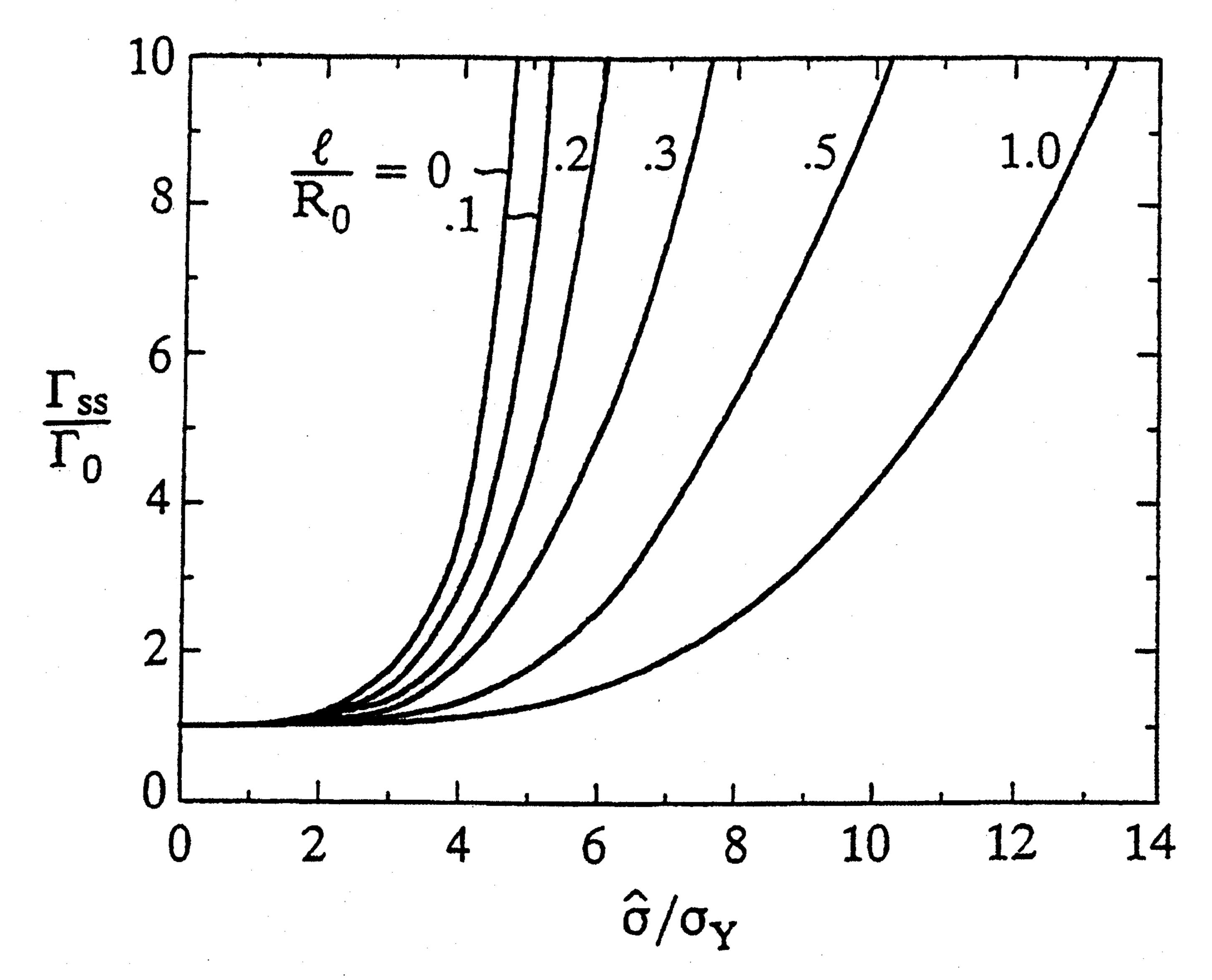


Figure 7. The influence of strain gradient hardening on Γ_{ss}/Γ_0 as predicted by the EPZ model for mode I growth in a homogeneous elastic-plastic solid characterized by J_2 SGP theory. The limit $\ell/R_0=0$ corresponds to conventional J_2 flow theory (Figure 3). The results are taken from Wei and Hutchinson (1997) and were computed with N=0.2, $\nu=0.3$, $\lambda_1=0.15$ and $\lambda_2=0.5$.

The influence of strain gradient hardening on Γ_{ss}/Γ_0 in the EPZ model appears through the dimensionless combination, ℓ/R_0 , such that for mode I crack growth, (2.12) becomes

$$\frac{\Gamma_{ss}}{\Gamma_0} = F_{\text{EPZ}} \left\{ \frac{\hat{\sigma}}{\sigma_Y}, N, \frac{\ell}{R_0} \right\}. \tag{4.2}$$

Curves of Γ_{ss}/Γ_0 as a function of $\hat{\sigma}/\sigma_Y$ for various values of ℓ/R_0 are displayed in Figure 7 for a homogeneous material with the tensile stress-strain curve (2.6) and a strain hardening index, N=0.2. The limiting curve for $\ell/R_0=0$ is that for the EPZ model based on conventional J_2 plasticity theory. The influence of the dimensionless parameter ℓ/R_0 on Γ_{ss}/Γ_0 is indeed large. At a given normalized peak separation stress $\hat{\sigma}/\sigma_Y$, Γ_{ss}/Γ_0 decreases sharply with increasing ℓ/R_0 . Whereas a crack in the conventional J_2 solid with N=0.2 is unable to achieve crack-tip stresses large enough to undergo separation if $\hat{\sigma}/\sigma_Y=5$, a crack in the J_2 SGP solid with $\ell/R_0 \geqslant 0.5$ achieves separation at normalized peak separation stresses twice that large.

The separation process determines whether strain gradient effects are likely to be important. Recall from (1.6) that R_0 is typically on the order of a fraction of a millimeter or more if the fracture process is void growth and coalescence. For such processes, ℓ/R_0 is much too small for gradient effects to influence crack growth. The length of the fracture process zone will be large compared to ℓ . By contrast, when the fracture process is atomic separation (c.f. (1.5)), ℓ and R_0 will often be comparable, and the strong gradient plasticity effects evident in Figure 7 should pertain.

The effect of ℓ/R_0 on the *unified model* is shown in Figure 8, again for the case of a mode I crack in a homogeneous solid with the tensile stress-strain curve (2.6) with N=0.2. Calculations for $\ell/R_0=0$ (conventional J_2 theory) are compared with those for a solid with $\ell/R_0=0.3$. As in the results just discussed, the only alteration to the unified model has been

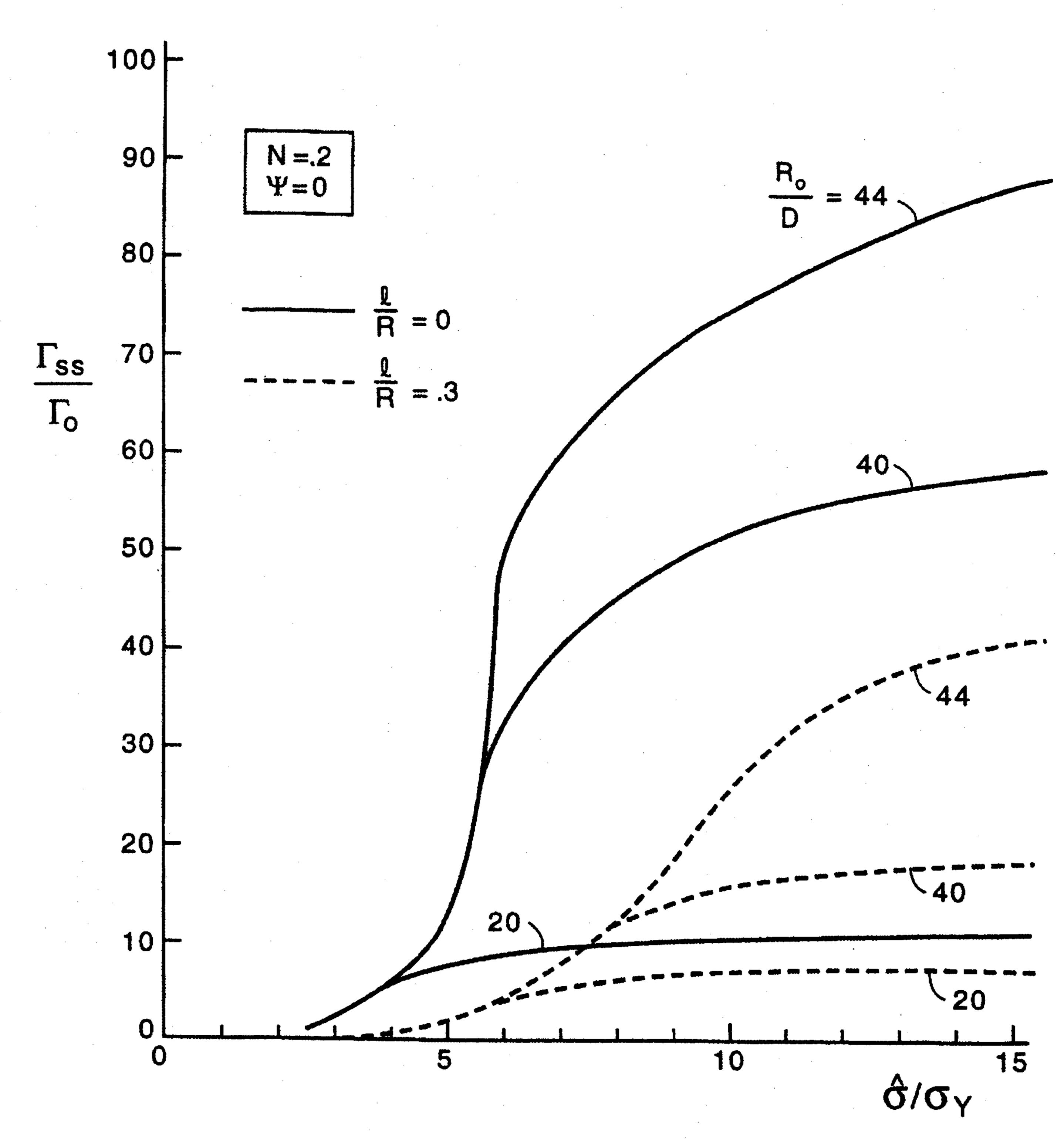


Figure 8. The influence of strain gradient hardening on Γ_{ss}/Γ_0 as predicted by the unified model for mode I growth in a homogeneous elastic-plastic solid characterized by J_2 SGP theory. The solid curves for $\ell/R_0=0$ coincide with the results for the conventional J_2 theory. The dashed curves are for the strain gradient theory with $\ell/R_0=0.3$. The calculations are made with $\nu=0.3$, $\lambda_1=0.15$ and $\lambda_2=0.5$.

to substitute J_2 SGP theory for the conventional J_2 theory as the constitutive theory characterizing the upper and lower half spaces. The effect of ℓ/R_0 on the macroscopic toughness prediction is similar to that noted for the EPZ model. Gradient hardening lowers the estimates of Γ_{ss}/Γ_0 , significantly so at large $\hat{\sigma}/\sigma_Y$ and R_0/D . The effect occurs across the whole range of the unified model, from the EPZ limit to the SSV limit. It should not be surprising that strain gradient hardening at the micron scale also plays an important role in determining macroscopic toughness in the SSV model. For atomic separation (c.f. (1.3)), the thickness D of the plasticity-free layer usually turns out to be much smaller than ℓ . Thus, material just outside the strip experiences gradient hardening, resulting in an elevation of traction levels acting on the plasticity-free strip, thereby altering the energy release rate at the crack tip. This is an effect that has been modeled by Lipkin et al. (1996) for crack growth initiation.

5. Discussion

Magnification of the work of interface separation due to plastic deformation in the region surrounding the crack tip depends on a fairly large set of parameters. Earlier work by Tvergaard and Hutchinson (1993) based on the EPZ model has shown that there is a strong dependence of Γ_{ss}/Γ_0 on ψ . Mixed mode toughness can be much larger than mode I toughness. Similar

trends are expected for the SSV and unified models. In the present work based on the unified model, there are four dimensionless parameters which are of primary importance in mode I

$$N, \frac{\hat{\sigma}}{\sigma_Y}, \frac{D}{R_0}, \frac{\ell}{R_0}. \tag{5.1}$$

While the interpretation of each of these dimensionless parameters is clear within the context of the unified model, a dependence on even three variables makes it difficult to connect the model to experiments (Bagchi and Evans, 1996; Evans et al., 1998). The situation for the fracture process of void nucleation, growth and coalescence simplifies considerably in this respect because the plasticity-free strip is irrelevant and $\ell/R_0 = 0$. The EPZ model, or equivalents (e.g. Rousselier et al., 1989; Xia and Shih (1995)), based on conventional plasticity theory is applicable. When the mechanism is atomic or molecular separation, the unified model helps to clarify of the limitations of the other models and provides guidance to the formulation of improved models. The following points summarize the most important implications of the unified model.

The interface strength, as measured by $\hat{\sigma}/\sigma_Y$, will generally be an important determinant of the total work of interface fracture when at least one of the solids deforms plastically. For atomistic separation processes, the work of separation Γ_0 and the interface strength $\hat{\sigma}$ are fundamental quantities which, in principle, can be computed using atomistic models (e.g. Raynolds et al., 1996). Both are affected by interface bonding conditions and interface segregants. Only when the length of the separation zone is small compared to the thickness of the plasticity-free strip will the interface strength cease to play a controlling role (c.f. Figures 5 and 6). This is the domain of validity of the SSV model. The length of the separation zone itself has a complicated dependence on $\hat{\sigma}/\sigma_Y$ and D/R_0 .

The plasticity-free strip of the SSV and unified models remains the most nebulous aspect of the models. The self-consistent arguments of Beltz et al. (1996) and Lipkin et al. (1996) for the determination of D provide insight into its validity as a region near the tip where continuum plasticity ceases to describe discrete dislocation interactions with each other and with the tip itself. The quantitative significant of the estimate of D by Beltz et al. (1996) can be questioned on the grounds that these authors use conventional plasticity to bridge between the continuum scale and the scale where discrete dislocation interactions become important. The strain gradient effects cited for deformations at the micron scale are likely to be equally important in the determination of D. On the other hand, even with uncertainties surrounding the identification of the plasticity-free strip, the unified model emphasizes its importance. Whether behavior close to the crack tip where any continuum plasticity description breaks down can be characterized by elastic behavior is open to question and certainly requires further validation. However, it is clear that a near-tip zone must exist within which continuum plasticity will be inadequate, if separation occurs at the atomic scale. The sensitivity of the predictions of the SSV and unified models to D provides evidence that this near-tip region, whether strictly elastic or not, has an important role to play in linking macroscopic toughness to separation at the atomic or molecular level.

The strong influence on macroscopic toughness of strain gradient hardening through the parameter ℓ/R_0 also serves to illustrate the importance of behavior at intermediate scales between macroscopic and microscopic. Given the recent body of experimental evidence on stress elevation due to straining in the presence of strain gradients at the micron scale, it is hard to imagine this effect does not make its presence felt at crack tip. Quantitative predictions

based on J_2 SGP theory reveal that the effects are indeed likely to be major if ℓ/R_0 is of order unity, as will usually be the case when the separation process is an atomistic one. This conclusion applies to all the models considered in this paper.

The unified model provides a framework for further modeling developments. The model relates macroscopic crack-growth behavior to the fundamental parameters characterizing the interface, Γ_0 and $\hat{\sigma}$. If accurate discrete dislocation models existed for describing plastic deformation, they might be used to completely replace continuum plasticity in the unified model. However, given the long and difficult history of first principles modeling of even the basic aspects of strain hardening, it seems unlikely that continuum plasticity could be supplanted by more basic dislocation mechanics in quantitative fracture models in the near future. To put this into perspective, consider that the plastic zone associated with a relatively tough interface can be as large as several hundred microns, containing as many as 10^5 dislocations. A more achievable goal might be to attempt further refinement of the 'plasticity-free' region using dislocation mechanics, continuing to rely on continuum plasticity outside this region. An approach along these lines might also enable the consideration of dislocation emission at the crack tip (Rice and Thomson, 1974), and its role in influencing the relation between macroscopic toughness and interface properties.

Acknowledgments

This work was supported in part by the Office of Naval Research under grant N00014-96-0559, by the National Science Foundation under Grant CMS-9634632, and by the Division of Engineering and Applied Sciences, Harvard University.

References

Bagchi, A. and Evans, A.G. (1996). The mechanics and physics of thin film decohesion and its measurement. *Interface Science* 3, 169–193.

Begley, M.R. and Hutchinson, J.W. (1998). The mechanics of size dependent indentation. To be published in *Journal of Mechanics and Physics of Solids*.

Beltz, G.E., Rice, J.R., Shih, C.F. and Xia, L. (1996). A self-consistent model for cleavage in the presence of plastic flow. Acta Materialia 44, 3943–3954.

Evans, A.G., Hutchinson, J.W. and Wei, Y. (1998). Interface adhesion: effects of plasticity and segregation. Harvard University Report MECH 337 (to be published in *Acta Materialia*).

Fleck, N.A. and Hutchinson, J.W. (1997). Strain gradient plasticity. *Advances in Applied Mechanics* 33, 295–361. Fleck, N.A., Muller, G.M., Ashby, M.F. and Hutchinson, J.W. (1994). Strain gradient plasticity: theory and experiment. *Acta Metallurgica et Materialia* 42, 475–487.

Lipkin, D.M., Clarke, D.R. and Beltz, G.E. (1996). A strain-gradient model of cleavage fracture in plastically deforming materials. *Acta Materialia* 44, 4051–4058.

Ma, Q. and Clarke, D.R. (1995). Size dependent hardness of silver single crystals. *Journal of Materials Research* 10, 853–863.

Needleman, A. (1987). A continuum model for void nucleation by inclusion debonding. *Journal of Applied Mechanics* 54, 525-531.

Nix, W.D. and Gao, H. (1998). Indentation size effects in crystalline materials: A law for strain gradient plasticity. Journal of Mechanics and Physics of Solids 46, 411–425.

Poole, W.J., Ashby, M.F. and Fleck, N.A. (1996). Micro-hardness of annealed and work-hardened copper polycrystals. Scripta Metallurgica et Materialia 34, 559–564.

Raynolds, J.E., Smith, J.E. Zhao, G.L. and Srolovitz, D.J. (1996). Physical Reviews B 53, 13883-13890.

Rice, J.R. (1988). Elastic fracture concepts for interfacial cracks. Journal of Applied Mechanics 55, 98–103.

Rice, J.R. and Thomson, R. (1974). Ductile vs. brittle behavior of crystals. Philosophical Magazine 29, 73–97.

- Rice, J.R., Suo, Z. and Wang, J.S. (1990). Mechanics and thermodynamics of brittle interfacial failure in bimaterial systems. In *Metal-Ceramic Interfaces*, (Edited by M. Ruhle, A.G. Evans, M.F. Ashby and J.P. Hirth), Pergamon Press, New York, 269–294.
- Rousselier, G., Devaux, J.-C., Mottet, G. and Devesa, G. (1989). A methodology for ductile fracture analysis based on damage mechanics: an illustration of a local approach of fracture. in *Nonlinear Fracture Mechanics: Vol. 11*, Elastic-Plastic Fracture, ASTM STP 995 (Edited by J.D. Landes, A. Saxena and J.G. Merkle) American Society of Testing Materials, Philadelphia, 332–354.
- Stelmashenko, N.A., Walls, M.G., Brown, L.M. and Milman, Y.V. (1993). Microindentations on W and Mo oriented single crystals: An STM study. Acta Metallurgica et Materialia 41, 2855–2865.
- Suo, Z., Shih, C.F. and Varias, A.G. (1993). A theory for cleavage cracking in the presence of plastic flow. Acta Metallurgica et Materialia 41, 1551–1557.
- Tvergaard, V. (1997). Cleavage crack growth resistance due to plastic flow around a near-tip dislocation-free region. Journal of Mechanics and Physics of Solids 45, 1007–1023.
- Tvergaard, V. and Hutchinson, J.W. (1992). The relation between crack growth resistance and fracture process parameters in elastic-plastic solids. *Journal of Mechanics and Physics of Solids* 40, 1377–1397.
- Tvergaard, V. and Hutchinson, J.W. (1993). The influence of plasticity on mixed mode interface toughness. *Journal of Mechanics and Physics of Solids* 41, 1119–1135.
- Wei, Y. and Hutchinson, J.W. (1997). Steady-state crack growth and work of fracture for solids characterized by strain gradient plasticity, *Journal of Mechanics and Physics of Solids* 45, 1253–1273.
- Xia, L. and Shih, C.F. (1995). Ductile crack growth I. A numerical study using computational cells with microstructurally-based length scales. *Journal of Mechanics and Physics of Solids* 43, 223–259.